Electronic Research Archive

ERA, 30(12): 4382–4400.
DOI: 10.3934/era.2022222
Received: 24 August 2022
Revised: 22 September 2022
Accepted: 28 September 2022
Published: 08 October 2022

http://www.aimspress.com/journal/era

Research article

Simulation of nonlinear characteristics of vertical vibration of railway freight wagon varying with train speed

Juping Yang[1,2], Junguo Wang[3,*] and Yongxiang Zhao[3]

[1] Traction Power State Key Laboratory, Southwest Jiaotong University, Chengdu 610031, China
[2] China Energy Group Railway Equipment Co., Ltd., Beijing 100011, China
[3] School of Mechanical Engineering, Southwest Jiaotong University, Chengdu 610031, China

* **Correspondence:** Email: jgwang@swjtu.edu.cn; Tel: +862887600690; Fax: +862887600690.

Abstract: Traditional vertical vibration models of rail vehicle usually have high degrees of freedom, which affects the efficiency of numerical simulation. Regardless of the coupling effect between the vehicle and rail, a six degree of freedom (6DOF) quarter model with vertical displacement and rotation angle is selected as the dynamic model. This accomplished by comparing the simulation results of half model and quarter model of the railway freight wagon, and the vertical vibration characteristics of the railway freight wagon when the wagon speed is changed. To further illustrate the nonlinear vibration characteristics and evolution laws of the car body and bogie frame of the freight wagon, the bifurcation diagrams, maximum Lyapunov exponent curves, axis trajectory curves, phase plane plots, Poincaré sections, and amplitude spectras are drawn and adopted to research the dynamic responses. The simulations reveal the complex vibration behavior such as periodic, quasi-periodic, multi-periodic, and chaotic motion. Some research results can help the industry to better design the speed limits of such railway freight wagons, and deeply understand or utilize the vertical vibration law of railway freight wagon in future research.

Keywords: railway freight wagon; modelling; nonlinear characteristics; chaos; Lyapunov exponent

1. Introduction

Railway freight transportation is developing toward large power and heavy loads, the research on railway freight car dynamics has become a research hotspot. With the development of railway speed-

up freight cars, the vibration response of the car body and bogie frame of the freight wagon also becomes more intense, which seriously affects the stability and safety of railway freight wagons. To reduce the violent vibration of railway vehicle caused by speeding operation of train, it is necessary to deeply understand the vibration characteristics of the car body and bogie frame of vehicle when freight train is in the sped-up state. The main methods to obtain the vibration characteristics of rail freight wagon are experimental methods and numerical simulation methods. Compared with the expensive cost of experiments, the numerical simulation methods can also obtain the vibration response of freight wagon efficiently, safely and cheaply. At present, many scholars have carried out a large number of studies on the dynamics of railway freight wagons.

Bruni et al. [1] summarized the application status of multi-body dynamics in railway vehicle dynamics, Iwnicki et al. [2] also summarized some improvements in the techniques used to simulate the dynamic behavior of a railway vehicle. To study the dynamic properties of the rail freight car under wheel flat condition, Ding et al. [3] established a railway wagon model with K6 bogie and studied the responses of wheel-rail forces and adapter vibration under flat fault. To study the dynamic behavior caused by wheel tread defects, Esteban et al. [4] modelled the wheel flat defect and introduced it into the multi-body dynamics simulation. Considering the vertical, pitch, and roll motions of the wagon system, Naeimi et al. [5] developed a model of the railway wagon and tested the dynamic characteristics under arbitrary track irregularity. Gialleonardo et al. [6] constructed a multibody model of a railway wagon and presented a numerical analysis of the steady-state solution reached after the transition through a curve. To study the influence of the wheel diameter difference on the wheel tread wear, Sui et al. [7] established a freight car model considering wheel-rail non-Hertzian contact. True and Asmund [8] also investigated the dynamic characteristics of a simple wheelset model, which supported one end of a freight car by springs with dry friction dampers. Zou et al. [9] improved a dynamic model by using polygonal contact model, in which the adjacent freight cars was incorporated into the longitudinal model of combined heavy haul trains, and the dynamic response of the coupler and its influence on the running safety were simulated. Hoffmann [10] analyzed the dynamic characteristics of European two-axle freight cars by using the multi-body model specially developed for UIC standard suspension.

Wheel-rail interaction of rail vehicle is an important research topic, Wu et al. [11] once modelled the railway vehicles in conventional longitudinal train dynamics as 2D models that considers suspensions and wheel-rail contact. Bian et al. [12] developed a 3D finite element model for the impact analysis induced by the wheel flat using ANSYS and investigated the effect of wheel flats on impact forces. Di et al. [13] analyzed the dynamic behavior of train sets and the impact of freight train composition on derailment risk and performed numerical simulations to determine the most critical conditions. Zhou et al. [14] adopted two types of container trucks to investigate the collision and derailment of railway trucks and found that the possibility of derailment was small when freight trains collided on a large radius curve. Xu et al. [15] presented a framework for modelling the railway freight car-ballast track interactions and established a motion equation by the linear and nonlinear characteristics of the system components. To analyze the dynamic characteristics of a heavy haul railway wagon in curve condition, Zhang et al. [16] built the freight wagon models by using ADAMS/Rail and VI-Rail. Meanwhile, the simulation was carried out on curve tracks with different radius. To study the dynamics of freight cars, Jozef et al. [17] adopted the training module to simulate the dynamic multicomponent system of UM software. Three-piece bogies with friction wedge suspensions are the most widely used bogies in heavy haul trains, and Wu et al. gave a review of dynamics modelling of friction wedge suspensions to improve general wagon dynamics simulations [18].

Proposing a methodology to optimize wedge suspensions using white-box suspension models, dynamic simulations of railway vehicle systems [19].

With the increase of freight cars length, the longitudinal dynamics become a key problem. Krishna et al. [20] developed a tool based on 3D multibody simulation to provide longitudinal compressive force limits and allowable longitudinal compressive force passing through curves. Based on the non-smooth dynamic theory, Oprea et al. [21] defined an alternative model for braking train, where the set-valued friction of Coulomb's law was considered, while Matej [22] analyzed the lateral dynamic behavior of a four-axle rail freight wagon with Union Internationale des Chemins de fer (UIC) suspension. Serajian et al. [23] investigated the length's effect on train dynamics during brake application, which was used in railways of Islamic Republic of Iran. Ghazavi and Taki [24] modelled a nonlinear system of freight car with two three-piece bogies, and the simulation results were compared with ADAMS/Rail model. Deng et al. [25] established a numerical model integrating fluid solid coupling, container loading model and high-speed freight train by LS-DYNA. Based on the rail vehicle–track coupling model, Zhai et al. [26] analyzed the dynamic impact of train speed increase on track structure. Rezvani and Mazraeh [27] studied the effects of wheel/rail friction coefficient and track curve radius on the nonlinear critical speed. By comparing the models of three piece and Y25 bogie, Kovalev et al. [28] discussed a numerical method of simulating the vehicle model in the presence of friction contact and gave the derailment safety analysis. Stichel [29] studied the nonlinearity of the two-axle freight car, especially the influence of friction damping on the running behavior of the freight wagon and gave the bifurcation curve and the limit cycle diagrams. Mark and Hans [30] investigated the nonlinear dynamics of a two-axle freight car with UIC suspension, Zhang et al. [31] proposed a new method to solve the large-scale vehicle-track coupling model with nonlinear wheel/rail contact, where the vehicle was treated as a multi-rigid body model, and the track was regarded as a three-layer beam model, and the numerical simulation examples demonstrated the accuracy of the proposed method.

As mentioned above, reviews of existing literatures show that many methods have been adopted to analyze the longitudinal and lateral dynamics of freight wagon, but the research on the influence of vertical vibration characteristics on rail freight wagon is relatively limited. The structural characteristics of railway freight wagons and the increase of running speed as well as other factors make the train generate complex vibration in the running process, which also has an important impact on the safety of the freight train. Ignoring the coupling effect between the vehicle and the track, how to apply the theory and method of large system to establish the vertical dynamic model of railway freight car body, bogie and wheel set coupling system, analyze and discover the vertical vibration law, and even make better use of the vibration characteristics is a research work with important engineering application value. At present, the traditional vertical vibration models of railway vehicle usually have high degrees of freedom, which affect the efficiency of numerical simulation. In this study, a 6DOF quarter model with vertical displacement and rotation angle is selected as the dynamic model by comparing the simulation results of half model and quarter model of the freight wagon, in which includes one car-body, two secondary suspensions, two bogie frames, four primary suspensions and four wheelsets. To further illustrate the nonlinear characteristics, the vertical vibration characteristics and evolution laws are analyzed by using bifurcation diagrams, maximum Lyapunov exponent curves, axis trajectory curves, phase plane plots, Poincaré sections, and amplitude spectras when the train speed is changed. The simulations reveal the complex vibration behavior such as periodic, quasi-periodic, multi-periodic, and chaotic motion. It is expected that the simulation data can provide a theoretical basis for designing the running speed of railway freight wagon, utilizing or controlling the dynamic behaviors of the freight wagon in the future.

This paper is organized as follows: Section 2 gives the modelling process of half model and quarter model of the railway freight wagon. Meantime the vibration responses of the two models are compared, and it is found that the difference between the simulations is very small. Based on the quarter model, the influences of train speed on the vertical vibration of car body and bogie frame are studied in Section 3. In the end the conclusions are summarized in Section 4.

2. Modelling of the railway freight wagon

2.1. Half model of the railway freight wagon

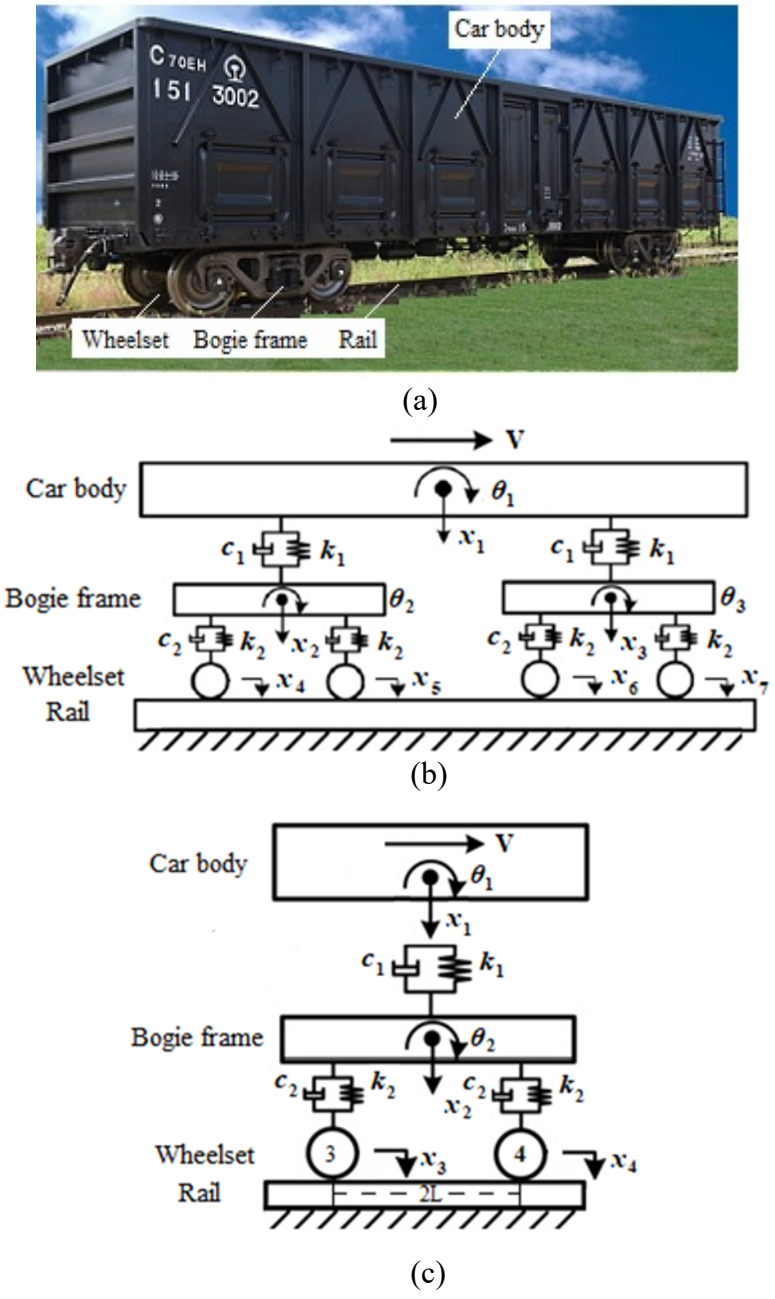

Figure 1. Dynamic model of railway freight wagon: (a) Photograph of railway freight; (b) Half model of rail freight wagon; (c) Quarter model of rail freight wagon.

A certain type of railway freight wagon has two bogies as shown in Figure 1(a), the vehicle model is considered as a multi-rigid body model which includes one car-body, two secondary suspensions, two bogie frames, four primary suspensions and four wheelsets. Figure 1(b) shows a half model of rail freight wagon, in which the car body and the bogie frame are assigned with vertical displacement and rotation angle, only the vertical displacement of the four wheelsets is considered. Therefore, there are ten degrees-of-freedoms (10DOF) in the half model without considering the coupling effect of vehicle and rail. The mechanical model of the proposed vehicle system can be expressed as follow:

$$M\ddot{X}+C\dot{X}+KX=H(F_g-F_w) \tag{1}$$

where M, C and K are the generalized mass, damping coefficient and stiffness coefficient matrices, respectively, $\ddot{X}$, $\dot{X}$ and X are generalized acceleration, velocity and displacement vectors, respectively. H is the sign matrix of the external forces, and its value is taken either 0 or 1, F_g and F_w are the gravity force and wheel/rail force, respectively.

If m_1, m_2 and m_3 are the masses of half of the car body, the left and right of bogie frame, m_4, m_5, m_6 and m_7 are the masses of four wheelsets in Figure 1(b), respectively, J_1, J_2 and J_3 are moments of inertia of car body, the left and right of bogie frame, respectively; k_1 and k_2 are the stiffness coefficients of secondary and primary suspensions, respectively, c_1 and c_2 are the damping coefficients of secondary and primary suspensions, respectively; x_1, x_2 and x_3 are the vertical displacements of the car body, the left and right of bogie frame, x_4, x_5, x_6 and x_7 are the vertical displacements of four wheelsets, respectively, θ_1, θ_2 and θ_3 are pitching rotations of car body, the left and right of bogie frame respectively, L and l are the distances between the two axles centres position of bogie frame and between the two bogie frame centres. In Eq (1), there exists the following formula

$$M=diag(m_1,J_1,m_2,J_2,m_3,J_3,m_4,m_5,m_6,m_7) \tag{2}$$

$$C=\begin{bmatrix}
2c_1 & 0 & -c_1 & 0 & -c_1 & 0 & 0 & 0 & 0 & 0\\
0 & 2c_1l^2 & c_1l & 0 & -c_1l & 0 & 0 & 0 & 0 & 0\\
-c_1 & c_1l & c_1+2c_2 & 0 & 0 & 0 & -c_2 & -c_2 & 0 & 0\\
0 & 0 & 0 & 2c_2L^2 & 0 & 0 & c_2L & -c_2L & 0 & 0\\
-c_1 & -c_1l & 0 & 0 & c_1+2c_2 & 0 & 0 & 0 & -c_2 & -c_2\\
0 & 0 & 0 & 0 & 0 & 2c_2L^2 & 0 & 0 & c_2L & -c_2L\\
0 & 0 & -c_2 & c_2L & 0 & 0 & c_2 & 0 & 0 & 0\\
0 & 0 & -c_2 & -c_2L & 0 & 0 & 0 & c_2 & 0 & 0\\
0 & 0 & 0 & 0 & -c_2 & c_2L & 0 & 0 & c_2 & 0\\
0 & 0 & 0 & 0 & -c_2 & -c_2L & 0 & 0 & 0 & c_2
\end{bmatrix} \tag{3}$$

$$K=\begin{bmatrix}
2k_1 & 0 & -k_1 & 0 & -k_1 & 0 & 0 & 0 & 0 & 0\\
0 & 2k_1l^2 & k_1l & 0 & -k_1l & 0 & 0 & 0 & 0 & 0\\
-k_1 & k_1l & k_1+2k_2 & 0 & 0 & 0 & -k_2 & -k_2 & 0 & 0\\
0 & 0 & 0 & 2k_2L^2 & 0 & 0 & k_2L & -k_2L & 0 & 0\\
-k_1 & -k_1l & 0 & 0 & k_1+2k_2 & 0 & 0 & 0 & -k_2 & -k_2\\
0 & 0 & 0 & 0 & 0 & 2k_2L^2 & 0 & 0 & k_2L & -k_2L\\
0 & 0 & -k_2 & k_2L & 0 & 0 & k_2 & 0 & 0 & 0\\
0 & 0 & -k_2 & -k_2L & 0 & 0 & 0 & k_2 & 0 & 0\\
0 & 0 & 0 & 0 & -k_2 & k_2L & 0 & 0 & k_2 & 0\\
0 & 0 & 0 & 0 & -k_2 & -k_2L & 0 & 0 & 0 & k_2
\end{bmatrix} \tag{4}$$

$$X = (x_1, \theta_1, x_2, \theta_2, x_3, \theta_3, x_4, x_5, x_6, x_7)^T \tag{5}$$

The wheel–rail force in Eq (1) can be described by the Hertzian theory, if $(x_{wi} - x_{ri} - x_{ii}) > 0$ then $F_{wi} = [(x_{wi} - x_{ri} - x_{ii})/G]^{3/2}$, else $F_{wi} = 0$. Here G is Hertzian coefficient, $G = 3.86R^{-0.115} \times 10^{-8}$, i = 1 and 2 indicate the first wheel-pair and the second wheel-pair, respectively, x_{wi} and x_{ri} are the vertical displacements of the wheelset and rail, respectively, and x_{ii} represents the track irregularity. The rail irregularity is described as an ideal cosine function as [31]

$$x_{ii}(t) = \frac{1}{2} a(1 - \cos\frac{2\pi V}{d} t) \tag{6}$$

where V is the running speed of railway freight train, a and d represent the wave depth and amplitude value of track irregularity, respectively, a = 11.2 mm and d = 10.8 m.

2.2. Quarter model of railway freight wagon

The car body and the bogie frame are assigned with vertical displacement and rotation angle, only the vertical displacement of the two wheelsets is considered. Without considering the coupling effect of vehicle and rail, there are six degrees-of-freedoms (6DOF) in the quarter model.

If m_1 and m_2 are the masses of quarter of the car body and bogie frame, m_3 and m_4 are the masses of left wheelset and right wheelset in Figure 1(c), respectively, J_1 and J_2 are moments of inertia of car body and bogie frame, respectively; k_1 and k_2 are the stiffness coefficients of secondary and primary suspensions, respectively, c_1 and c_2 are the damping coefficients of secondary and primary suspensions, respectively. x_1, x_2, x_3 and x_4 are the vertical displacements of the car body, bogie frame, left wheelset and right wheelset, respectively, θ_1 and θ_2 are pitching rotations of car body and bogie frame, respectively, L and l are the distances between the two axles centres position of bogie frame and between the two bogie frame centres. In Eq (1), there exists the following formula

$$M = diag(m_1, J_1, m_2, J_2, m_3, m_4) \tag{7}$$

$$C = \begin{bmatrix} 2c_1 & 0 & -c_1 & 0 & 0 & 0 \\ 0 & 2c_1 l^2 & c_1 l & 0 & 0 & 0 \\ -c_1 & c_1 l & c_1 + 2c_2 & 0 & -c_2 & -c_2 \\ 0 & 0 & 0 & 2c_2 L^2 & c_2 L & -c_2 L \\ 0 & 0 & -c_2 & c_2 L & c_2 & 0 \\ 0 & 0 & -c_2 & -c_2 L & 0 & c_2 \end{bmatrix} \tag{8}$$

$$K = \begin{bmatrix} 2k_1 & 0 & -k_1 & 0 & 0 & 0 \\ 0 & 2k_1 l^2 & k_1 l & 0 & 0 & 0 \\ -k_1 & k_1 l & k_1 + 2k_2 & 0 & -k_2 & -k_2 \\ 0 & 0 & 0 & 2k_2 L^2 & k_2 L & -k_2 L \\ 0 & 0 & -k_2 & k_2 L & k_2 & 0 \\ 0 & 0 & -k_2 & -k_2 L & 0 & k_2 \end{bmatrix} \tag{9}$$

$$X = (x_1, \theta_1, x_2, \theta_2, x_3, x_4)^T \tag{10}$$

The calculation formulas of the wheel–rail force and rail irregularity are the same as that of half model mentioned above.

3. Influence of train speed on vertical vibration of car body and bogie frame

3.1. Comparison of two vertical vibration models

Table 1. Parameters of system simulation.

Parameters	Values
Mass of the car body (kg)	9.03×10^5
Pitch moment of inertia of the car body (kg m^2)	9.84×10^7
Mass of the bogie frame (kg)	1575
Pitch moment of inertia of the bogie frame (kg m^2)	257
Mass of the wheelset (kg)	1100
Stiffness of the primary suspension (N/m)	2.5×10^7
Damping of the primary suspension (N s/m)	4.36×10^4
Stiffness of the secondary suspension (N/m)	5.87×10^6
Damping of the secondary suspension (N s/m)	2.25×10^4
Distance between the two bogie frame centers (m)	8.20
Distance between two axles of bogie frame (m)	1.80
Wheelset rolling radius (m)	0.42
Rail mass per unit length (kg/m)	60.64
Sleeper spacing (m)	0.545
Sleeper width (m)	0.273
Mass of half sleeper (kg)	125.5

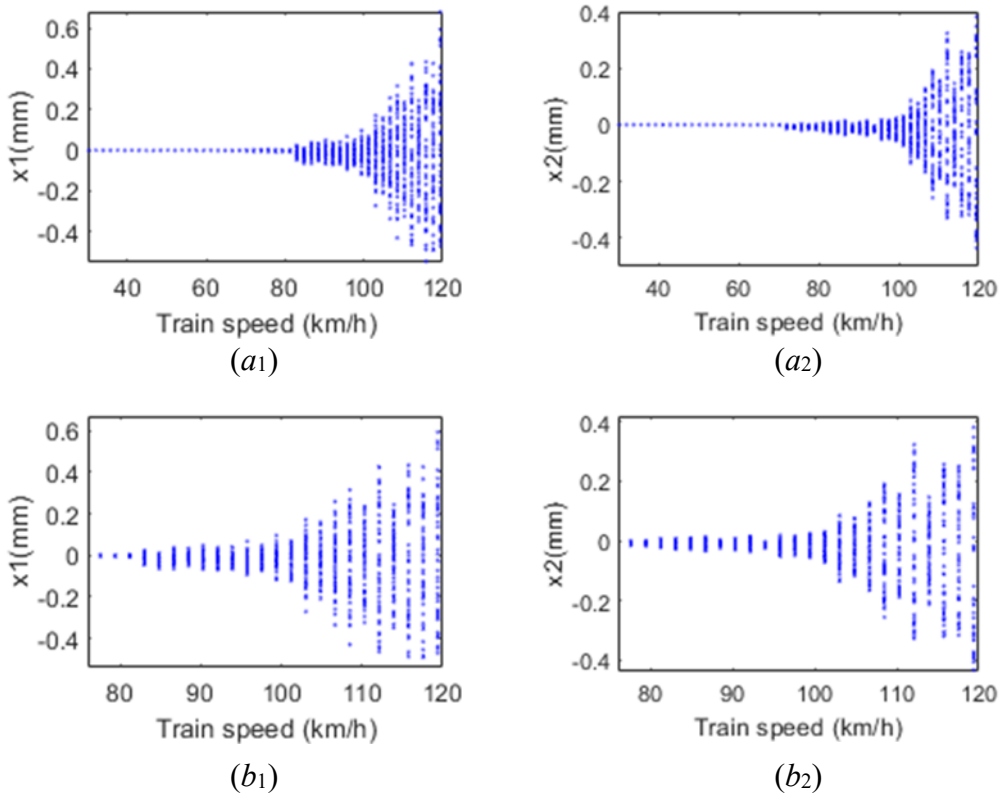

Figure 2. Bifurcation diagrams of vertical displacement of car body and bogie frame for half model. (a) Global bifurcation diagram; (b) Local bifurcation diagram.

Based on the half model and quarter model of the car body and bogie frame, the Runge-kutta method is adopted to solve the system equation, and some simulation parameters are given in Table 1.

Figures 2(a) to 3(a) illustrate the global bifurcation diagrams of vertical displacement of the car body and bogie frame for half model and quarter model when the train speed is changed. For the proposed railway freight wagon, the designed maximum running speed of the train is 120 km/h, hence, Figures 2(b) to 3(b) illustrate the local bifurcation diagrams for two models. It can be seen that the vertical displacement of both models is very small when the speed is less than 75 km/h, in which the maximum vertical displacement of the car body and bogie frame for half car model is less than 0.03 and 0.02 mm, while the corresponding displacement of quarter model is less than 0.04 and 0.02 mm, respectively.

With the increase of the train speed, the vertical vibration displacement also increases, but the errors of the two models are very small too and can be ignored. For instance, when train speed equals 90 km/h and 120 km/h respectively, the maximum vertical displacement of car body and bogie frame for half model is 0.12 and 0.05 mm, 0.65 and 0.45 mm, while the corresponding displacement of quarter model is about 0.14 and 0.055 mm, 0.6 and 0.4 mm, respectively. Since the simulation time of drawing bifurcation diagram of the quarter model (t = 16,247 s) is far less than that of the half model (t = 25,936 s), the quarter model above is then selected as the vertical vibration model of the railway freight wagon in this study.

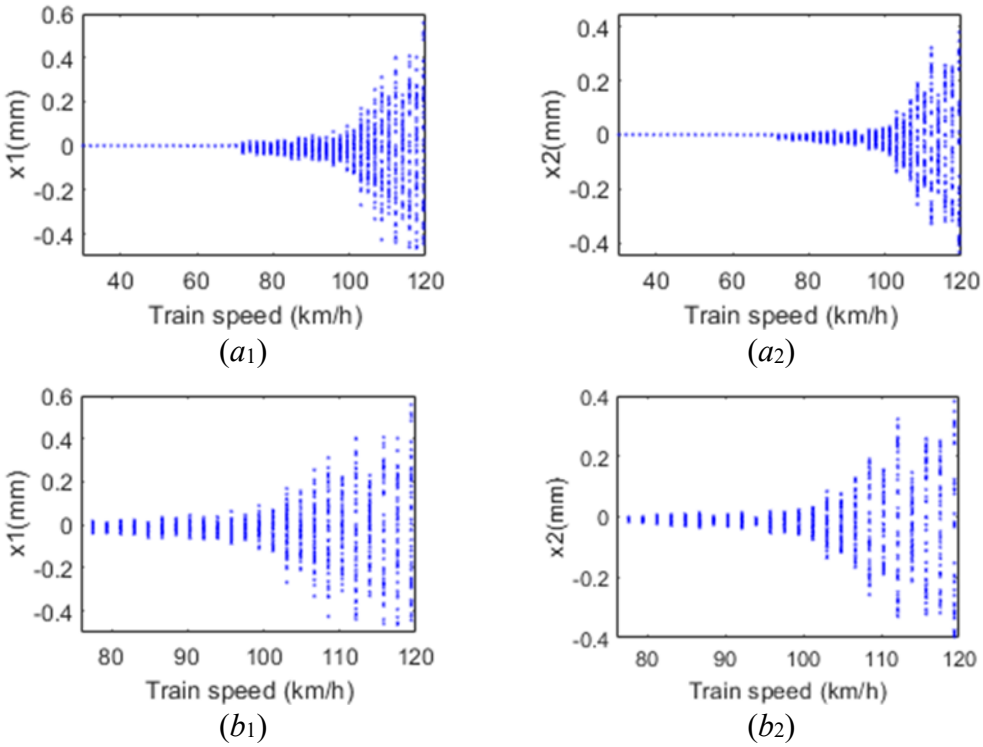

Figure 3. Bifurcation diagrams of vertical displacement of car body and bogie frame for quarter model. (a) Global bifurcation diagram; (b) Local bifurcation diagram.

3.2. Nonlinear vertical vibration characteristics of the quarter model

To further illustrate the nonlinear characteristics of vertical vibration of car body and bogie frame for the quarter model, Figure 4 shows the maximum exponential curve of the car body and bogie frame varying with train speed. Meantime, Figures 5–10 also display the nonlinear vertical vibration

responses of the car body and bogie frame. Here, a_1, b_1, c_1 and d_1 represent the dynamic response of the car body in the x_1 direction, a_2, b_2, c_2 and d_2 represent the dynamic response of the bogie frame in the x_2 direction, respectively. As shown in Figures 3 and 5, when the train speed does not exceed 75 km/h, i.e., V = 70 km/h, Poincaré section has a single point, phase plane diagram is only one closed circle, time domain response diagram shows a sine wave, and amplitude-frequency spectrum has only one peak amplitude, hence the system responses of the car body and bogie frame enter stable period-1 motion. Where the Lyapunov exponents are negative, and the maximum vertical displacement of the car body and bogie frame is very small, which is approximately equal to 0.04 and 0.02 mm, respectively.

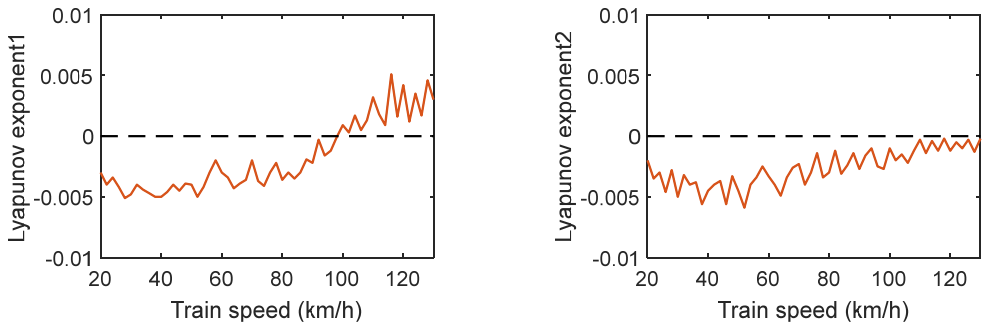

(*a*) (*b*)

Figure 4. Maximum Lyapunov exponent diagram of quarter model varying with train speed: (*a*) Car body; (*b*) Bogie frame.

In Figure 5 and other figures below, the units of displacement x1 and x2, velocity dx1 and dx2 are mm and mm/s, and the units of time t and frequency f are second (s) and hertz (Hz) respectively.

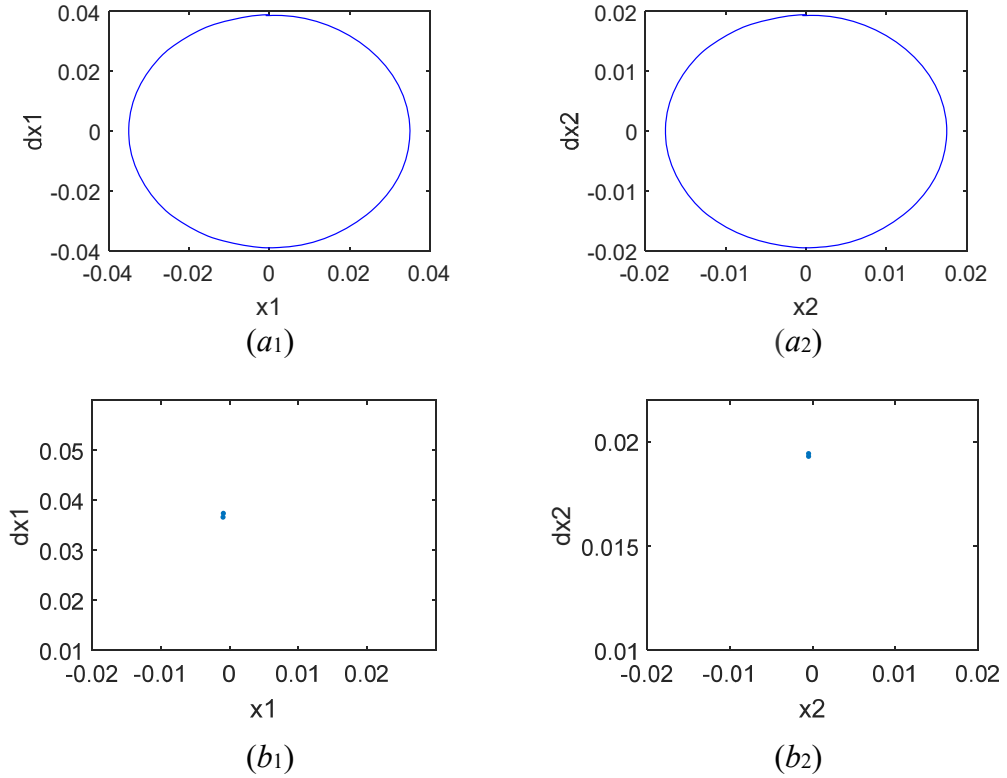

(a_1) (a_2)

(b_1) (b_2)

Continued on next page

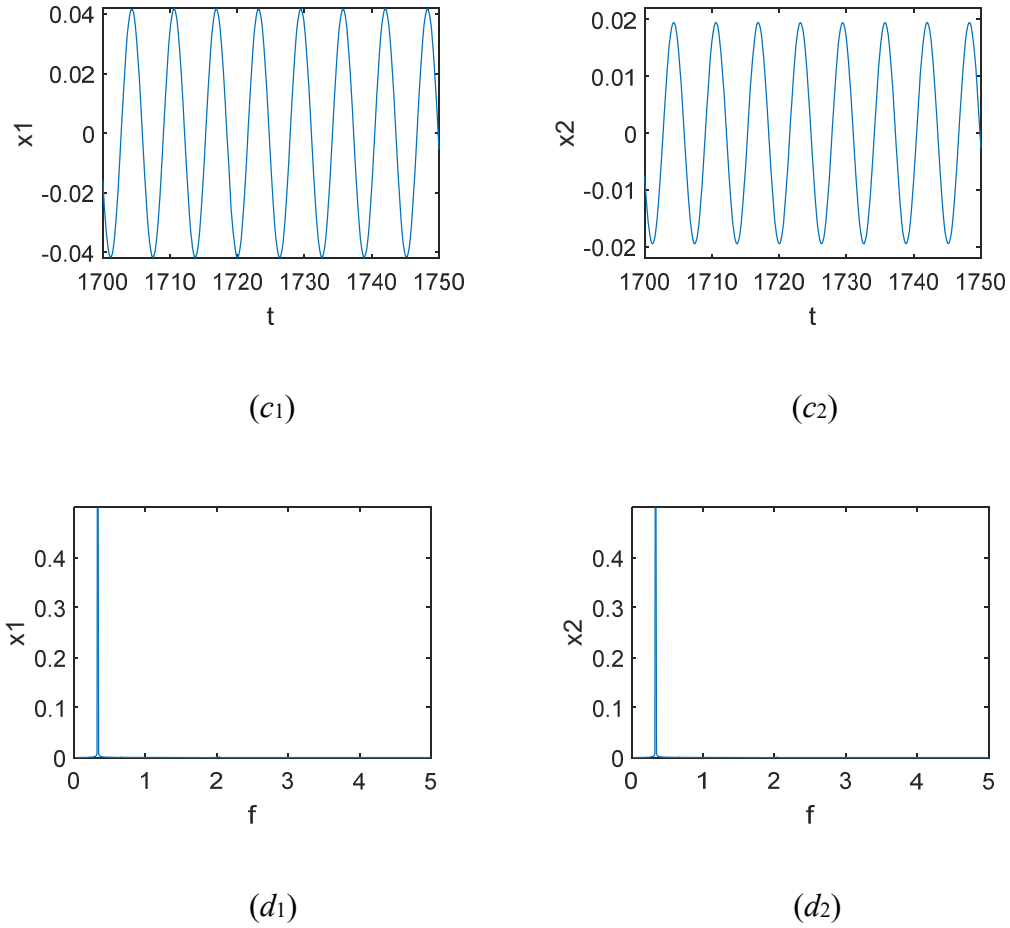

Figure 5. Dynamic response of car body and bogie frame when V = 70 km/h: (a) Phase plane plot; (b) Poincaré section; (c) Axis trajectory curve; (d) Amplitude spectra.

With the increase of wagon speed, the vibration responses of car body and bogie frame have changed significantly. When the speed V = 75 km/h, the vertical vibration responses of the car body and bogie frame leave period-1 motion, enter periodic-6 motion and periodic-4 motion, respectively. As displayed in Figure 6, six and four return points are shown in the Poincaré maps, respectively, phase plane diagrams have six and four closed circles, time domain response diagrams show a period motion, and the amplitude-frequency spectrums reveal numerous excitation frequencies, hence the vertical vibration responses of the car body and bogie frame are period-6 and period-4 motion, respectively, in which the Lyapunov exponents are negative, and the maximum vertical displacements of car body and bogie frame have almost no change.

When wagon speed continues to increase, i.e., V = 85 km/h, the vertical vibration responses of the car body and bogie frame enter multi-periodic motion. As displayed in Figure 7, eighteen return points are shown in Poincaré sections, phase plane diagrams have multiple closed circles, time domain response diagrams show multi-period motion, and amplitude-frequency spectrums also reveal numerous excitation frequencies. It is obvious that the vertical vibration response of the freight wagon is multi-periodic motion. Meanwhile the Lyapunov exponents are negative, and the maximum vertical displacements of the car body and bogie frame increase to about 0.05 and 0.022 mm.

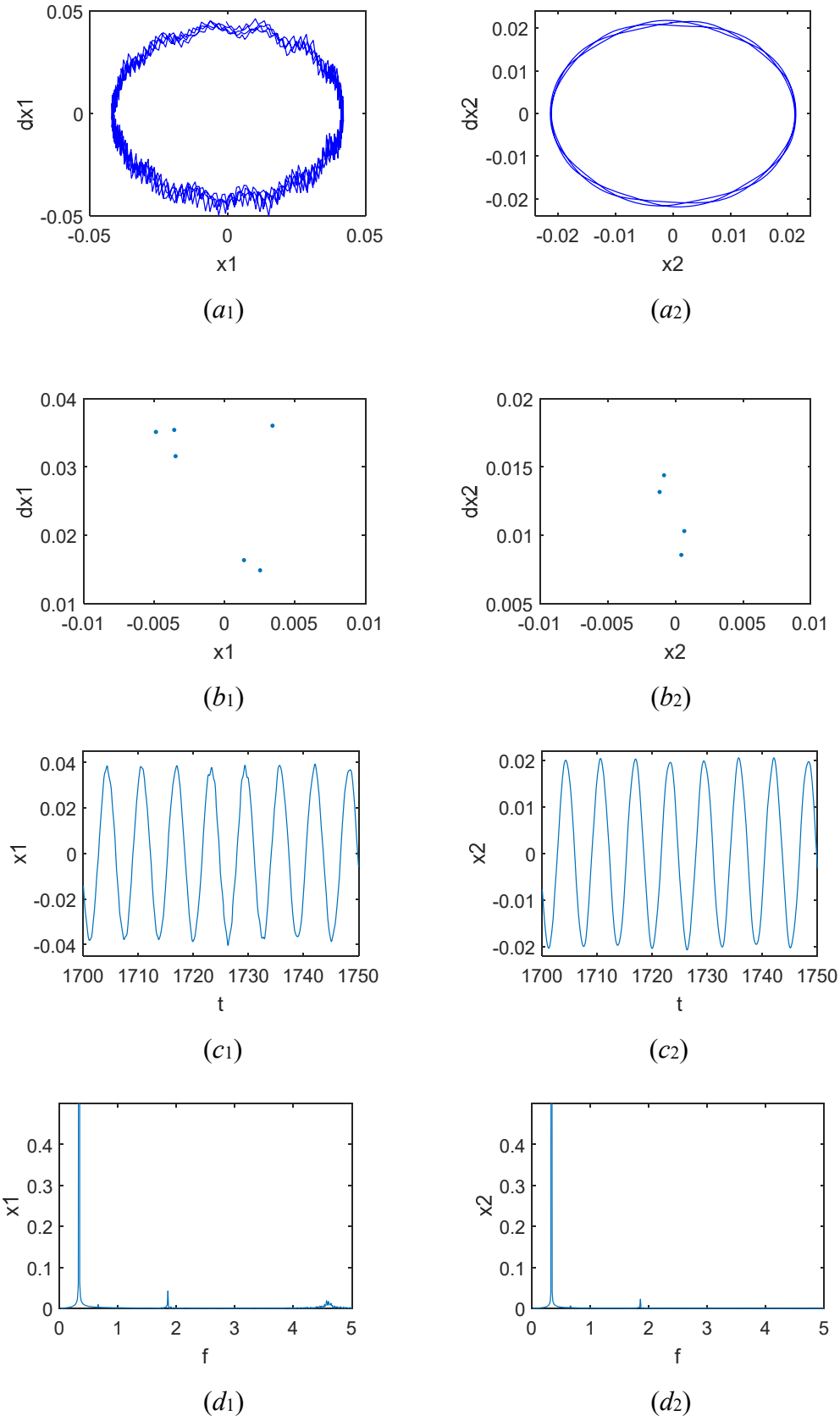

Figure 6. Dynamic response of the car body and bogie frame when V = 75 km/h: (a) Phase plane plot; (b) Poincaré section; (c) Axis trajectory curve; (d) Amplitude spectra.

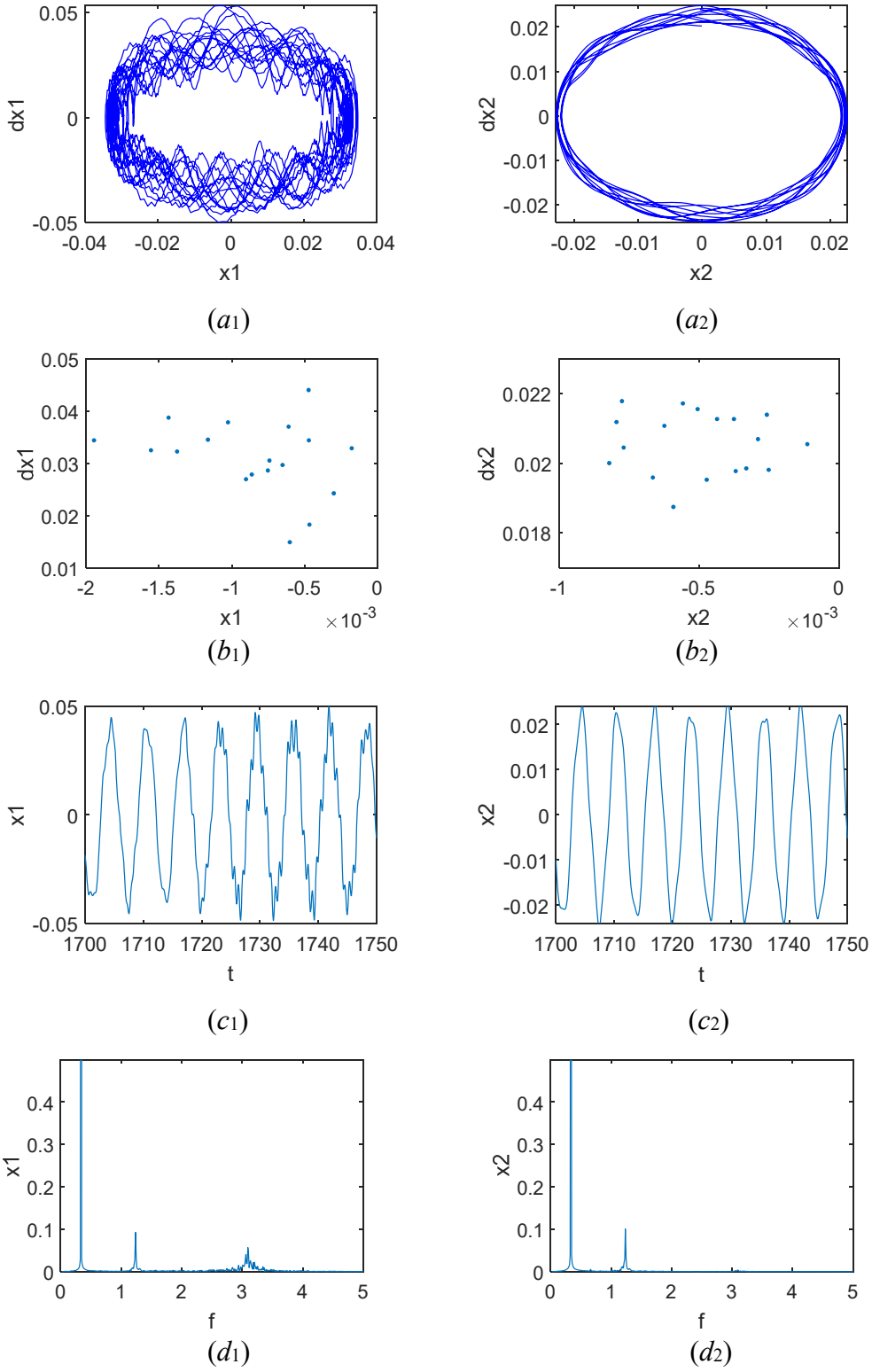

Figure 7. Dynamic response of the car body and bogie frame when V = 85 km/h: (a) Phase plane plot; (b) Poincaré section; (c) Axis trajectory curve; (d) Amplitude spectra.

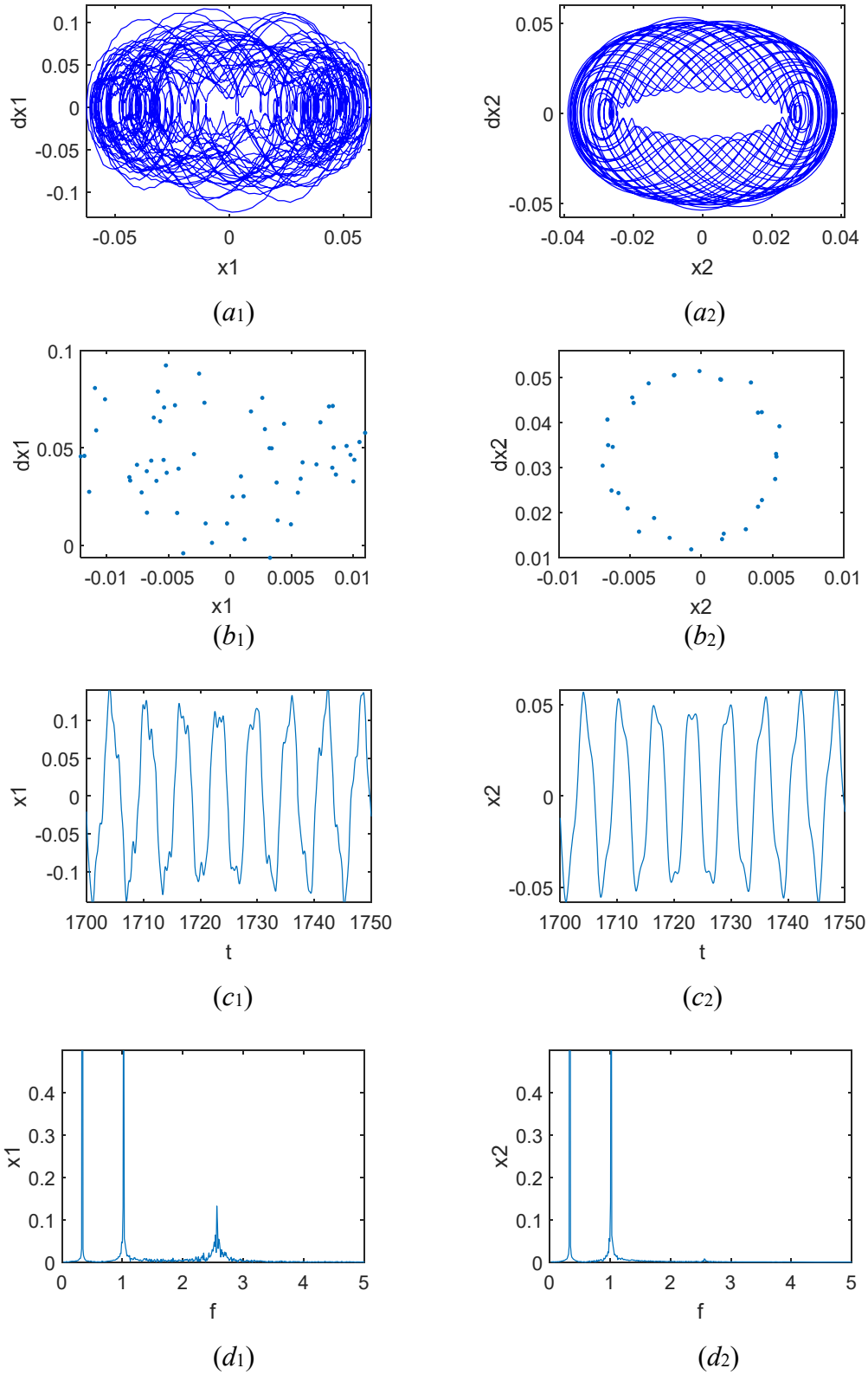

Figure 8. Dynamic response of the car body and bogie frame when V = 100 km/h: (a) Phase plane plot; (b) Poincaré section; (c) Axis trajectory curve; (d) Amplitude spectra.

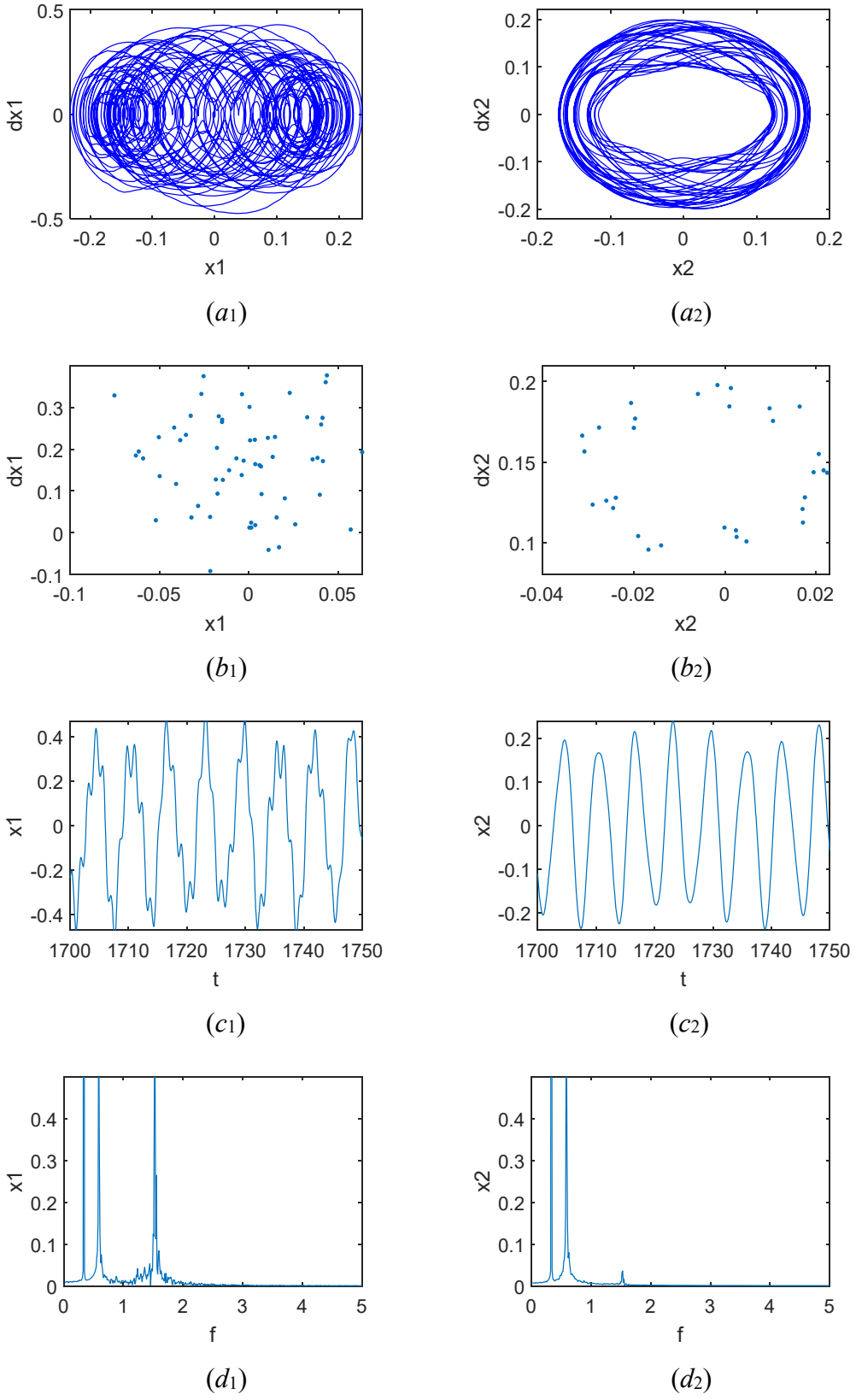

Figure 9. Dynamic response of the car body and bogie frame when V = 110 km/h: (a) Phase plane plot; (b) Poincaré section; (c) Axis trajectory curve; (d) Amplitude spectra.

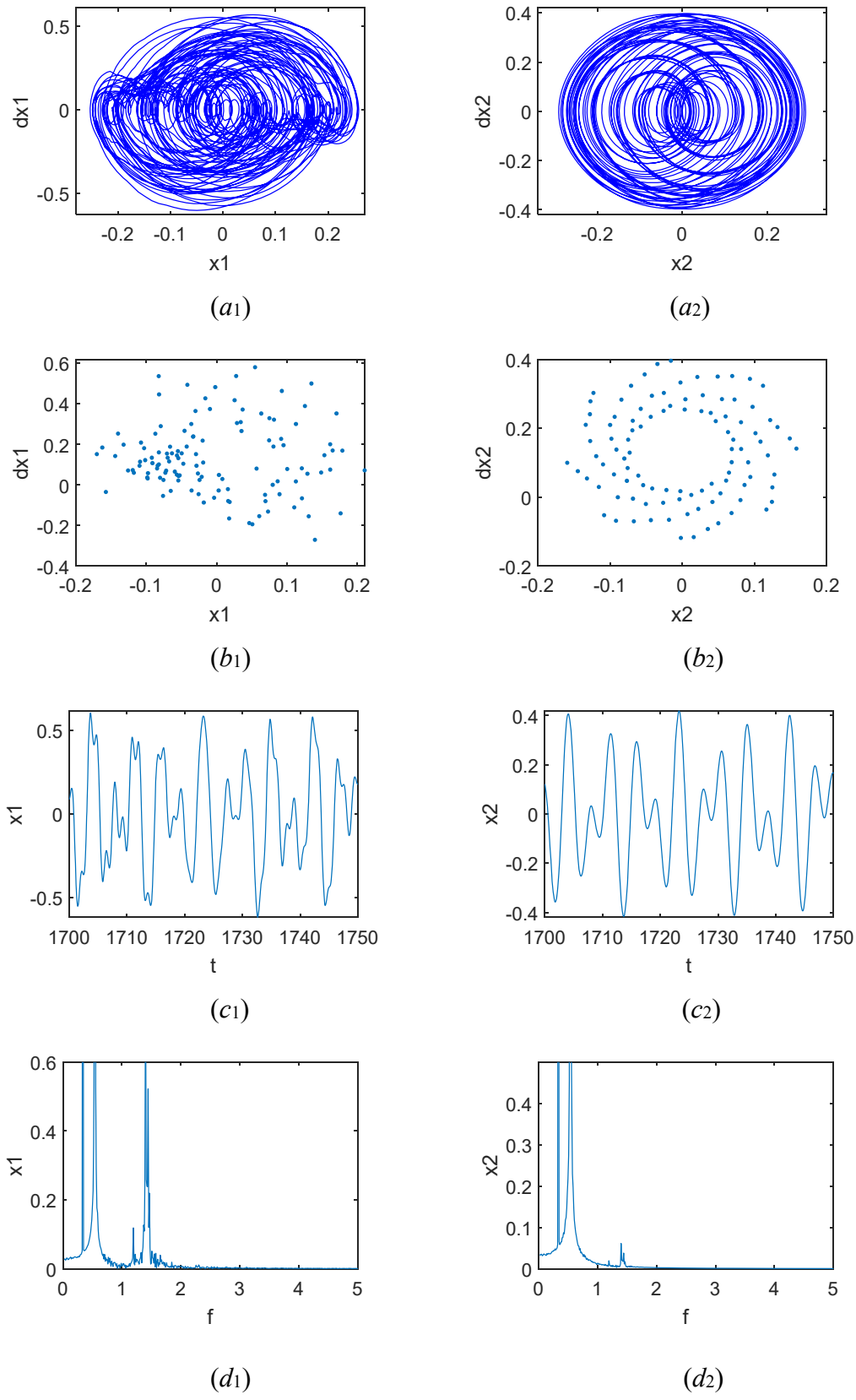

Figure 10. Dynamic response of the car body and bogie frame when V = 120 km/h: (a) Phase plane plot; (b) Poincaré section; (c) Axis trajectory curve; (d) Amplitude spectra.

The nonlinear wheel rail contact forces exist in the system model, which is the reason for the nonlinear vertical vibration of the wagon system. Especially when the wagon speed increases to 100 km/h, chaos occurs in the wagon system, and the vertical vibration amplitude also increases. As seen in Figure 8, the vertical vibration responses of the car body and bogie frame contain chaotic state and quasi period motion, respectively. As shown in Figure 4(a), the Lyapunov exponent of the car body is positive, and in Figure 8(a1)–(d1), the Poincaré section shows the finite points, phase plane curve and axis trajectory curve are closed, and amplitude spectrum is discrete, the vertical vibration response of the car body is then regarded as chaotic motion. At the same time, the Lyapunov exponent of the bogie frame is negative as shown in Figure 4(b), the phase plane curve becomes regular, and the attractor of Poincaré section has closed curve as displayed in Figure 8(a2)–(d2), it is clear that the vertical vibration response of bogie frame is only the quasi-periodic motion, not chaotic motion. On the other hand, with the increase of train speed, the vertical vibration amplitude of the car body and bogie frame obviously began to increase, and the maximum vertical displacements of the car body and bogie frame, x_1 and x_2, increase to close to 0.14 and 0.055 mm, respectively.

4. Conclusions

The vertical dynamic model mainly studies the vibration performance of railway freight wagon in the vertical plane during the operation, so that the vertical vibration can be reduced or controlled in future research. Without considering the coupling effect of vehicle and rail, a 6DOF generalized mass model with vertical displacement and rotation angle is established, which includes one car-body, two secondary suspensions, two bogie frames, four primary suspensions and four wheelsets. The nonlinear vertical vibration characteristics and evolution laws of the car body and bogie frame are analyzed by using bifurcation diagrams, maximum Lyapunov exponent curves, axis trajectory curves, phase plane plots, Poincaré sections, and amplitude spectras when the train speed is changed. The simulations reveal the complex vibration behavior of the railway freight car such as periodic, quasi-periodic, multi-periodic, and chaotic motion. Some conclusions can be summarized as follows:

Since the simulation time of the quarter model is far less than that of the half model, and the difference between the simulation results of the quarter model and the half model is very small, therefore, the 6DOF quarter model can replace the half model as the vertical vibration dynamic model of the railway freight wagon.

When the wagon speed is not greater than 75 km/h, the Lyapunov exponents are negative, the vertical vibration responses of the car body and bogie frame is in stable period-1 motion, and the corresponding vertical vibration displacement is also very small, especially when V = 70 km/h, the maximum vibration displacement is equal to 0.04 and 0.02mm, respectively. For the proposed railway freight wagon, the designed maximum running speed of the train is 120 km/h, hence the recommended running speed of the railway freight wagon can be chosen near 70 km/h.

The nonlinear wheel rail contact forces exist in the system model, which is the reason for the nonlinear vertical vibration of the wagon system. Especially when the wagon speed increases to 100 km/h, chaos occurs in the wagon system, and the vertical vibration amplitude also increases. Meanwhile, with the increase of the wagon speed, the vertical vibration of the car body and bogie frame undergoes the changes from multi-period to the chaotic motion and from multi-period to quasi period motion, respectively. When wagon speed equals 85, 10, 110 and 120 km/h, respectively, the vertical amplitude of the car body is 0.05, 0.1, 0.42 and 0.6 mm, while the vertical amplitude of the bogie frame is relatively small, which is equal to 0.022, 0.055 mm, 0.22 to 0.4 mm respectively.

Therefore, as the wagon speed increases, the vertical vibration of the car body must be monitored in real time.

Acknowledgments

The work was supported by Sichuan Science and Technology Program (No. 2020YFH0080), National Natural Science Foundation of China (51475439), and the Science and technology innovation project of Shenhua Railway Freight Car Transportation Co., Ltd (SHGF-13-77). The authors thank them for financial support. The authors also would like to thank the reviewers for their valuable comments.

Conflict of interest

The authors declare there is no conflict of interest.

References

1. S. Bruni, J. P. Meijaard, G. Rill, A. L. Schwab, State-of-the-art and challenges of railway and road vehicle dynamics with multibody dynamics approaches, *Multibody Syst. Dyn.*, **49** (2020), 1–32. https://doi.org/10.1007/s11044-020-09735-z
2. S. D. Iwnicki, S. Stichel, A. Orlova, M. Hecht, Dynamics of railway freight vehicles, *Veh. Syst. Dyn.*, **53** (2015), 995–1033. https://doi.org/10.1016/j.jsv.2018.12.033
3. C. R. Ding, X. Y. Peng, Q. S. Wang, Research on dynamic characterization of railway freight car under wheel flat condition (in Chinese), *Mech. Sci. Tech. Aero. Eng.*, **40** (2021), 1279–1284. https://doi.org/10.13433/j.cnki.1003-8728.20200205
4. B. Esteban, S. Maksym, S. C. Colin, Wheel flat detectability for Y25 railway freight wagon using vehicle component acceleration signals, *Veh. Syst. Dyn.*, **58** (2020), 1893–1913. https://doi.org/10.1080/00423114.2019.1657155
5. M. Naeimi, J. A. Zakeri, M. Shadfar, M. Esmaeili, 3D dynamic model of the railway wagon to obtain the wheel-rail forces under track irregularities, *Proc. Inst. Mech. Eng. Part F: J. Multibody Dyn.*, **229** (2015), 357–369. https://doi.org/10.1177/1464419314566833
6. E. D. Gialleonardo, S. Bruni, H. True, Analysis of the nonlinear dynamics of a 2-axle freight wagon in curves, *Veh. Syst. Dyn.*, **52** (2014), 125–141. https://doi.org/10.1080/00423114.2013.863363
7. S. Q. Sui, K. Y. Wang, L. Ling, Z. G. Chen, Effect of wheel diameter difference on tread wear of freight wagons, *Eng. Fail. Anal.*, **127** (2021), 1873–1961. https://doi.org/10.1016/j.engfailanal.2021.105501
8. H. True, R. Asmund, The dynamics of a railway freight wagon wheelset with dry friction damping, *Veh. Syst. Dyn.*, **38** (2002), 149–163.
9. R. M. Zou, S. H. Luo, W. H. Ma, Simulation analysis on the coupler behaviour and its influence on the braking safety of locomotive, *Veh. Syst. Dyn.*, **56** (2018), 1747–1767. https://doi.org/10.1080/00423114.2018.1435893
10. M. Hoffmann, On the dynamics of European two-axle railway freight wagons, *Nonlinear Dyn.*, **52** (2008), 301–311. https://doi.org/10.1007/s11071-007-9279-1

11. Q. Wu, C. Cole, M. Spiryagin, Train braking simulation with wheel-rail adhesion model, *Veh. Syst. Dyn*., **58** (2020), 1226–1241. https://doi.org/10.1080/00423114.2019.1645342
12. J. Bian, Y. T. Gu, H. M. Martin, A dynamic wheel-rail impact analysis of railway track under wheel flat by finite element analysis, *Veh. Syst. Dyn*., **51** (2013), 784–797. https://doi.org/10.1080/00423114.2013.774031
13. G. E. Di, G. Cazzulani, S. Melzi, F. Braghin, The effect of train composition on the running safety of low-flatcar wagons in braking and curving manoeuvres, *Proc. Inst. Mech. Eng. Part F: J. Rail Rapid Transit*., **231** (2017), 666–677. https://doi.org/10.1177/0954409716636923
14. H. C. Zhou, J. Zhang, M. Hecht, Three-dimensional derailment analysis of crashed freight trains, *Veh. Syst. Dyn*., **52** (2014), 341–361. https://doi.org/10.1080/00423114.2014.881512
15. L. Xu, X. M. Chen, X. W. Li, X. L. He, Development of a railway wagon-track interaction model: case studies on excited tracks, *Mech. Syst. Signal Pr*., **100** (2018), 877–898. https://doi.org/10.1016/j.ymssp.2017.08.008
16. D. Zhang, D. B. Clarke, Y. Peng, H. Gao, C. J. Dong, Effect of the combined centre of gravity on the running safety of freight wagons, *Veh. Syst. Dyn*., **57** (2019), 1271–1286. https://doi.org/10.1080/00423114.2018.1494841
17. S. Jozef, J. Marek, W. Dariusz, Modelling the longitudinal dynamics of long freight trains on broad gauge metallurgical railway line, *Procedia Eng*., **192** (2017), 840–844. https://doi.org/10.1016/j.proeng.2017.06.145
18. Q. Wu, C. Cole, M. Spiryagin, Y. Q. Sun, A review of dynamics modelling of friction wedge suspensions, *Veh. Syst. Dyn*., **52** (2014), 1389–1415. http://dx.doi.org/10.1080/00423114.2014.943249
19. Q. Wu, Y, Sun, M. Spiryagin, C. Cole, Methodology to optimize wedge suspensions of three-piece bogie of railway vehicles, *J. Vib. Control*., **24** (2018), 565–581. https://doi.org/10.1177/1077546316645698
20. V. V. Krishna, M. Berg, S. Stichel, Tolerable longitudinal forces for freight trains in tight S-curves using three-dimensional multi-body simulations, *Proc. Inst. Mech. Eng. Part F: J. Rail Rapid Transit*., **234** (2020), 454–467. https://doi.org/10.1177/0954409719841794
21. R. A. Oprea, C. Cruceanu, M. A. Spiroiu, Alternative friction models for braking train dynamics, *Veh. Syst. Dyn*., **51** (2013), 460–480. https://doi.org/10.1080/00423114.2012.744459
22. J. Matej, A new mathematical model of the behaviour of a four-axle freight wagon with UIC single-link suspension, *Proc. Inst. Mech. Eng. Part F: J. Rail Rapid Transit*., **225** (2011), 637–647. https://doi.org/10.1177/0954409711398173
23. R. Serajian, S. Mohammadi, A. Nasr, Influence of train length on in-train longitudinal forces during brake application, *Veh. Syst. Dyn*., **57** (2019), 192–206. https://doi.org/10.1080/00423114.2018.1456667
24. M. R. Ghazavi, M. Taki, Dynamic simulations of the freight three-piece bogie motion in curve, *Veh. Syst. Dyn*., **46** (2008), 955–973. https://doi.org/10.1080/00423110701730737
25. G. Deng, Y. Peng, C. Yan, B. Wen, Running safety evaluation of a 350 km/h high-speed freight train negotiating a curve based on the arbitrary Lagrangian-Eulerian method, *Proc. Inst. Mech. Eng. Part F: J. Rail Rapid Transit.*, **235** (2021), 1143–1157. https://doi.org/10.1177/0954409720986283

26. W. M. Zhai, Q. C. Wang, Z. W. Lu, X. S. Wu, Dynamic effects of vehicles on tracks in the case of raising train speeds, *Proc. Inst. Mech. Eng. Part F: J. Rail Rapid Transit*., **215** (2001), 125–135. https://doi.org/10.1243/0954409011531459
27. M. A. Rezvani, A. Mazraeh, Dynamics and stability analysis of a freight wagon subjective to the railway track and wheelset operational conditions, *J. Mec. Theor. Appl.*, **61** (2017), 22–34. https://doi.org/10.1016/j.euromechsol.2016.08.011
28. R. Kovalev, N. Lysikov, G. Mikheev, D. Pogorelov, V. Simonov, V. Yazykov, et al., Freight car models and their computer-aided dynamic analysis, *Multibody Syst Dyn.*, **22** (2009), 399–423. https://doi.org/10.1007/s11044-009-9170-6
29. S. Stichel, Limit cycle behaviour and chaotic motions of two axle freight wagons with friction damping, *Multibody Syst Dyn*, **8** (2002), 243–255. https://doi.org/10.1023/A:1020990128895
30. H. Mark, T. Hans, The dynamics of European two-axle railway freight wagons with UIC standard suspension, *Veh. Syst. Dyn.*, **46** (2019), 225–236. https://doi.org/10.1080/00423110801935848
31. J. Zhang, Q. Gao, S. J. Tan, W. X. Zhong, A precise integration method for solving coupled vehicle-track dynamics with nonlinear wheel-rail contact, *J. Sound Vib*., **331** (2012), 4763–4773. https://doi.org/10.1016/j.jsv.2012.05.033

AIMS Press